Multi-objective distributed generation integration in radial distribution system using modified neural network algorithm

Ali Tarraq, Faissal El Mariami, Abdelaziz Belfqih

Laboratory of Energy and Electrical Systems, Department of Electrical Engineering, Ecole Nationale Supérieure d'Electricité et de Mécanique, Hassan II University of Casablanca, Casablanca, Morocco

Article Info	ABSTRACT
	This paper introduces a new approach based on a chaotic strategy and a neural network algorithm (NNA), called chaotic-based NNA (CNNA), to solve the optimal distributed generation allocation (ODGA), in the radial distribution system (RDS). This consists of determining the optimal locations and sizes of one or several distributed generations (DGs) to be inserted into the RDS to minimize one or multiple objectives while meeting a set of security limits. The robustness of the proposed method is demonstrated by applying it to two different typical RDSs, namely IEEE 33-bus and 69-bus. In this regard, simulations are performed for three DGs in the cases of unity power factor (UPF) and optimal power factor (OPF), considering single and multi-objective optimization, by minimizing the total active losses and improving the voltage profile, voltage deviation (VD) and voltage stability index (VSI). Compared to its original version and recently reported methods, the CNNA solutions are more competitive without increasing the complexity of the optimization algorithm, especially when the RDS size and problem dimension are extended. *This is an open access article under the [CC BY-SA](#) license.*

Corresponding Author:

Ali Tarraq
Laboratory of Energy and Electrical Systems, Department of Electrical Engineering, Ecole Nationale
Supérieure d'Electricité et de Mécanique, Hassan II University of Casablanca
B.P 8118, Oasis, Casablanca, Morocco
Email: ali.tarraq@gmail.com

1. INTRODUCTION

During this period of rising prices, mainly caused by the severe acute respiratory syndrome coronavirus 2 (SARS-CoV-2) pandemic and the conflict between Russia and Ukraine, the grid integration of renewable distributed generation (RDG) in the radial distribution system (RDS), is one of the most sustainable alternatives considered by the majority of countries in the world [1]. For developing countries such as Morocco, this type of source allows, for the best, to reach energy independence and transition [2]. RDG's integration allows for achieving the desired development and mitigating the economic damage resulting from this global crisis.

According to the literature, distributed generation (DG) based on renewable sources is a small-scale production unit exploiting renewable energy resources (such as solar, wind, water, biomass, or geothermal energy), close to the point of use, where the users are the producers-whether they are individuals, small businesses and/or a local community. If DGs are also connected (to share surplus power), they become a local renewable energy network, also called a microgrid. Which in turn can be connected to similar networks nearby [3], [4].

Depending on the nature of the power supplied, DGs are classified into three categories [5]:
− Type 1: Generates active power only unity power factor distributed generation (UPF-DG).
− Type 2: Generates reactive power only (zero power factor (PF)).

−   Type 3: Generates active power and reactive power (lagging PF).

In addition to helping reduce greenhouse gas emissions, the integration of RDG into the RDS improves the controllability and overall efficiency of the system and increases the rate of benefit [6]. However, due to the complexity of the distribution system, the location and/or random sizing of these sources can harm the overall system performance and parameters [7]. For this reason, the insertion of DGs with renewable sources requires an optimization study, often referred to as the optimal DG allocation (ODGA) in the RDS. Typically, ODGA is used to find the optimal location and size of one or several DGs to be integrated, to improve the overall performance of the RDS, by subjecting to a set of constraints related to voltage, current, and power [8].

However, the interdependence between the parameters of the RDS as well as its size makes the ODGA a combinatorial, and multimodal problem, whose solution is too hard to be done using conventional and analytical methods [8]. In this context, most researchers have proven the effectiveness of metaheuristic methods for solving ODGA. These methods are inspired by the innate behavior developed in living beings, or by physical and natural phenomena such as gravitation [9]. Due to their random nature, this type of method does not depend on the initial solution, as are conventional methods, e.g., linear or non-linear programming. Therefore, these methods are quite robust, as they can generate good-quality solutions with reduced algorithmic complexity.

During the last seven years, metaheuristic optimization methods have attracted more attention from researchers and investors for solving the ODGA problem. Muthukumar and Jayalalitha [10] proposed the hybridization of the harmonic search algorithm (HSA) and the particle artificial bee colony algorithm (PABCA), to find the sizes and locations of two different DGs simultaneously with capacitor banks in the typical IEEE 33-bus and 119-bus RDSs, to reduce the power losses and improve the voltage profile. Ali *et al.* [11] have successfully proved the effectiveness of hybridizing the ant-lion optimizer (ALO) and a loss sensitivity factor (LSF)-based method, to solve the ODGA. The study focuses on the insertion of a hybrid photovoltaic (PV)-wind-DG in 34-bus and 69-bus networks, to improve the voltage profile and stability, and to reduce the active power losses with variable load models. Literature [12] demonstrates the superiority of comprehensive teaching and learning-based optimization (CTLBO) over quasi-oppositional TLBO (QOTLBO). This method, implemented for the IEEE 33-bus, 69-bus, and 118-bus networks, is used to reduce losses, improve voltage profile, and save annual consumption in the cases of variable and constant load, with three UPF-DGs. The research paper [13] proposes a comparative study between tabu search algorithm (TSA), scatter search algorithm (SSA), and ant colony optimization (ACO). These three algorithms are applied for the same network (IEEE 13-bus) to minimize the active losses through the optimal integration of three DGs at different PFs. The study shows that the SSA gives the best results, while the worst are provided by the ACO. In [14], a Chao and quasi-opposition (QOC) strategy are adopted to improve the exploration and exploitation capability of the symbiotic organism search (SOS) algorithm, to be able to solve the ODGA problem. The proposed algorithm aims to reduce the active losses and improve the profile and stability of the voltage by optimally integrating three DGs with fixed and optimal PF, in the typical 33-bus, 69-bus and 118-bus networks. In [15], the same authors merged SOS and neural network algorithm (NNA) to allocate, simultaneously, three DGs and three capacitor banks (CBs) within the two IEEE 33-bus and IEEE 69-bus networks, adopting a constant and a variable load models. The study focuses on minimizing a multi-objective function with five weighted objectives, namely, the index of active losses, voltage deviation, voltage stability, power supply reliability, and load balance.

According to the latest literature, the NNA in its original version can provide competitive results, since it has a good operating capability. However, it is still limited in terms of exploration [15]. It is true that mixing the NNA with another method with good exploration capacity, such as the SOS, improves the results obtained, but this considerably increases the complexity of the algorithm and the number of tuning parameters. In this context, the present study proposes the improvement of the global search capacity of the NNA by adopting a Chao strategy, based on the logistic map. As such, the proposed method is referred to as the chaotic-based neural network algorithm (CNNA) and is used to solve the ODGA problem for the optimal insertion of three DGs at different PFs. The effectiveness of CNNA is tested for two different networks, namely IEEE 33-bus and IEEE 69-bus, in single-objective, and multi-objective contexts, by minimizing three indices such as active loss index (ALI), voltage deviation index (VDI), and global voltage stability index (GVSI). The results obtained by CNNA are compared with those obtained by SOS-NNA in [15], and other existing methods such as quasi-oppositional chaotic symbiotic organisms search (QOCSOS) [14], and sine cosine algorithm (SCA) [16].

This paper comprises three other sections. The next one describes the adopted formulation of the ODGA problem, namely the details of the multi-objective function and the constraints involved. The third section presents a description of the CNNA framework. Section 4 includes a discussion and a comprehensive analysis of the obtained results. Then, the different limitations and perspectives of the study are presented in the conclusion section.

2. POBLEM FORMULATION

2.1. Active loss index

The calculation of total active losses, noted P_l, is a crucial step in determining the efficiency and performance of the RDS. This is done through a well-established formula that considers various electrical parameters such as current, voltage, and resistance in the RDS. In (1) is specifically designed to provide an accurate estimate of the energy losses due to resistive heating within the system. This information is valuable for optimizing the RDS and ensuring that it operates at peak performance.

$$P_l = \sum_{i=1}^{N_L} R_i I_i^2 \tag{1}$$

where N_L presents the total number of branches, I_i and R_i denote respectively the branch current and resistance of line number i. Subsequently, the ALI can be expressed as (2):

$$ALI = \frac{P_{l_{wDG}}}{P_{l_{woDG}}} \tag{2}$$

where Pl_{woDG} and Pl_{wDG} represent the total real losses without and with DG insertion.

2.2. Voltage deviation index

The voltage deviation (VD) presents the total offset between the nodal voltages and the base voltage, which is also the voltage at the reference node of the network. It is expressed as (3):

$$VD = \sum_{i=1}^{N_b} (V_i - V_{ref})^2 \tag{3}$$

where N_b shows the total number of nodes in the network. While V_{ref} indicates the reference voltage, which is equal to 1 per unit (pu), and V_i presents the voltage at node number i. Accordingly, the VDI can have the following formula:

$$VDI = \frac{VD_{wDG}}{VD_{woDG}} \tag{4}$$

where VD_{woDG} and VD_{wDG} represent the VD before and after DG insertion.

The reduction of the VDI significantly affects the voltage profile of the RDS. The process involves bringing the set of nodal voltages closer to the base voltage, which acts as a reference point at the slack bus. This results in a more uniform voltage profile, with the nodal voltages being closer to the reference value. The improvement in the voltage profile leads to a more stable and efficient RDS, which is essential for maintaining reliable power supply. The base voltage acts as a benchmark, ensuring that the voltage deviations are within acceptable limits and reducing the risk of voltage-related problems such as power outages, surges, or drops. Overall, the reduction of VDI is a critical step in ensuring the reliability and stability of RDS.

2.3. Global voltage stability index

The voltage stability index VSI quantifies the ability of a node to resist against strong voltage drops. For load flow to be possible, the VSI of each node in the network must be strictly positive [17]. The VSI of a node n of the RDS depends on the voltage at node m upstream n, such that [18]:

$$VSI(n) = |V_m|^4 - 4[P_n X_{m,n} - Q_n R_{m,n}]^2 - 4[P_n R_{m,n} + Q_{i+1} X_{m,n}]|V_n|^2 \tag{5}$$

where $R_{m,n}$ and $X_{m,n}$ are the line resistance and the line reactance of the branch linked between nodes m and n, P_n and Q_n are respectively, the active and reactive power exiting from node n, such that:

$$P_n + j \times Q_n = (V_n \times I_{m,n})^* \tag{6}$$

where j is an imaginary number such that j² = -1 and $I_{m,n}$ is the current flowing through the line (m,n). It has the following expression:

$$I_{m,n} = \frac{V_m - V_n}{R_{m,n} + j X_{m,n}} \tag{7}$$

where V_m and V_n present the voltage at node m and node n respectively.

The objective of maximizing the minimum VSI is to improve the overall stability of a power distribution network. To achieve a more stable network, the minimum VSI must be maximized, which requires finding the optimal operating point that balances network stability and power flow. Herein, the GVSI can be used to quantify the stability of the entire network and can be expressed according to (8). By maximizing the GVSI, the stability and reliability of the power distribution network can be improved, ensuring a consistent and uninterrupted power supply to customers.

$$GVSI = \frac{\min(VSI_{woDG})}{\min(VSI_{wDG})} \qquad (8)$$

where VSI_{woDG} and VSI_{wDG} indicate the VSI without and with the three DGs respectively.

2.4. Multi-objective function (MOF)

Generally, the MOF is formulated to address multiple objectives simultaneously. As a weighted sum, the MOF represents the optimization problem's objectives and the trade-off between them. The weights assigned to each objective represent their relative importance, and the MOF can be optimized to find the best solution that balances these objectives. This approach provides a more comprehensive and flexible way to address complex optimization problems and can lead to better decision-making and more efficient solutions. In this study, the MOF can be expressed as (9):

$$Min\ MOF = w_1 ALI + w_2 VDI + w_3 GVSI + \sum p_i \qquad (9)$$

where w_1, w_2, and w_3 are weighting coefficients such that $w_1 + w_2 + w_3 = 1$. In a single-objective context, the only function chosen is the PLI since the power losses are the most important parameter in the case of RDS. Herein, the weighting coefficients are respectively equal to 1, 0, and 0. In the multi-objective context, these coefficients are chosen to be 0.3, 0.5, and 0.2 respectively. This choice is due to the huge number of executions realized. In (9), p_i coefficients present the penalty factors that serve as a support mechanism for the considered constraints.

For each constraint, a p_i factor is associated. If the chosen solution does not respect one of the constraints, then the corresponding p_i takes the value 100. Thus, the optimization program automatically rejects the corresponding solution, and the search space is limited.

2.5. Constraints

In order to ensure that the solutions reached for the RDS comply with normal operation, a set of security limits are established. These limits are in place to guarantee that the solutions do not compromise the stability or performance of the RDS. These security limits include voltage limits, thermal limits, DG capacity limits, PF limits, and DG location constraints, and are defined as (10):

− Voltage limits

$$V_{min} \leq |V_i| \leq V_{max} \qquad (10)$$

− Thermal limits

$$I_l \leq I_{limit} \qquad (11)$$

− DG capacity limits

$$P_{DG_{min}} \leq P_{DG_i} \leq P_{DG_{max}} \qquad (12)$$

$$0.1\ P_L \leq \sum_{i=1}^{N_{dg}} P_{DG_i} \leq 0.75\ P_L \qquad (13)$$

− PF limits

$$0.8 \leq PF_g \leq 1 \qquad (14)$$

− DG location constraint

$$2 \leq DG_{loc} \leq N_b \qquad (15)$$

where V_{min} and V_{max} are the limit values of the nodal voltage and V_i is the voltage at the ith node, I_l is the line current at the branch l, and I_{limit} its maximum value. Powers P_{DGi} and Q_{DGi} are respectively active and reactive power of the DG number i, and P_L denotes the total power demand. Moreover, PF_g presents the power factor of DG number g, and N_{dg} is the total number of DGs.

3. CNNA FRAMEWORK

The NNA is inspired by the biological way in which the nervous system and neural networks function in living beings [19]. It is similar to the artificial neural network (ANN) method that is often used in prediction studies. Typically, ANN aims to reduce the difference between the given target value and the predicted value by adjusting weight factors. The only difference between the two methods is that for the NNA the target value is considered as an output, while for the ANN it is part of the inputs of the algorithm.

To improve the ability of the exploration in the NNA, a chaotic strategy is joined to it. As a result, the CNNA framework consists of five components. The first one consists in updating the N positions of an X_t matrix in each iteration t, according to the following formula:

$$X_{t+1} = X_t * [1 + W_t] \tag{16}$$

where W_t presents the $N \times N$ matrix of weights such that:

$$\sum_{i=1}^{N} W_t(k,l) = 1 \qquad 0 < W_t(k,l) < 1, \quad k = 1,2,..N, \quad l = 1,2...N \tag{17}$$

The second step of the NNA is the update of W_t according to (17):

$$W_{t+1}(k) = W_t(k) + 2\gamma.\left[W_{target} - W_t(k)\right] \qquad k = 1,2,...,N \tag{18}$$

where γ is a random number uniformly chosen between 0 and 1, and W_{target} presents the vector of weights corresponding to the best position.

The third operator aims to improve the capacity of the global search of the NNA. It is called the bias operator, which depends on a modification factor β. In each iteration, β is updated according to the following formula:

$$\beta_{t+1} = 0.99\beta_t \tag{19}$$

Once this operator is executed, the bias of X_t and W_t is done according to (20) and (21):

$$X_{q,P} = lb_{i,P} + \left(ub_{q,P} - lb_{q,P}\right) \otimes rand_{q,P} \qquad q = 1,2,..,N \tag{20}$$

$$W_w = rand_w \tag{21}$$

where ub and lb present, respectively the upper and lower bounds of the decision variables, $rand$ is a random number uniformly chosen between 0 and 1 and $\otimes$ symbolizes the element-wise product. While, P is the vector of indices of the N_p decision variables that must be biased, and w presents the vector of indices of N_w number of weights to be biased such that:

$$N_p = round(D \times \beta_t) \tag{22}$$

$$N_w = round(N \times \beta_t) \tag{23}$$

where D presents the problem dimension or the total number of decision variables.

To improve the local search capability, a fourth component is incorporated to the NNA, which is called the transfer operator. If the bias operator is not executed, then this operator is performed to change the positions X_t according to the following:

$$N_w = \left[X_{target} - X_t(k)\right] \qquad k = 1,2,...,N \tag{24}$$

$$X_{t+1}(k) = X_t(k) + 2\gamma'\left[X_{target} - X_t(k)\right] \qquad k = 1,2,...,N \tag{25}$$

where γ' is a random number between 0 and 1, X_{target} denotes the best position found so far, and $X_t(k)$ is the kth position at the tth iteration.

According to (19), β_t decreases with the number of iterations, which decreases the chance of performing the bias operator. This significantly decreases the exploration capability of the NNA. To cope with this problem, in this study, a fifth component is added to the NNA. It is a Chao strategy based on the logistic map, which is the most adopted in the literature. It consists of generating a set of β values according to (24):

$$\beta_{t+1} = \lambda\beta_t(1 - \beta_t) \qquad t = 1,2,\dots,t_{max} \tag{26}$$

where t_{max} the maximum number of iterations and λ is the Chao factor, considered equal to 4. The initial value of β_t is randomly chosen according to the uniform distribution between 0 and 1.

Thus, (19) is not adopted for the modification of the bias factor in the main CNNA framework. Rather, a number N_p of β factors are generated in the initialization step according to (24). Obviously, this does not affect the time and space complexity of the optimization program. The flowchart of the CNNA is shown in Figure 1.
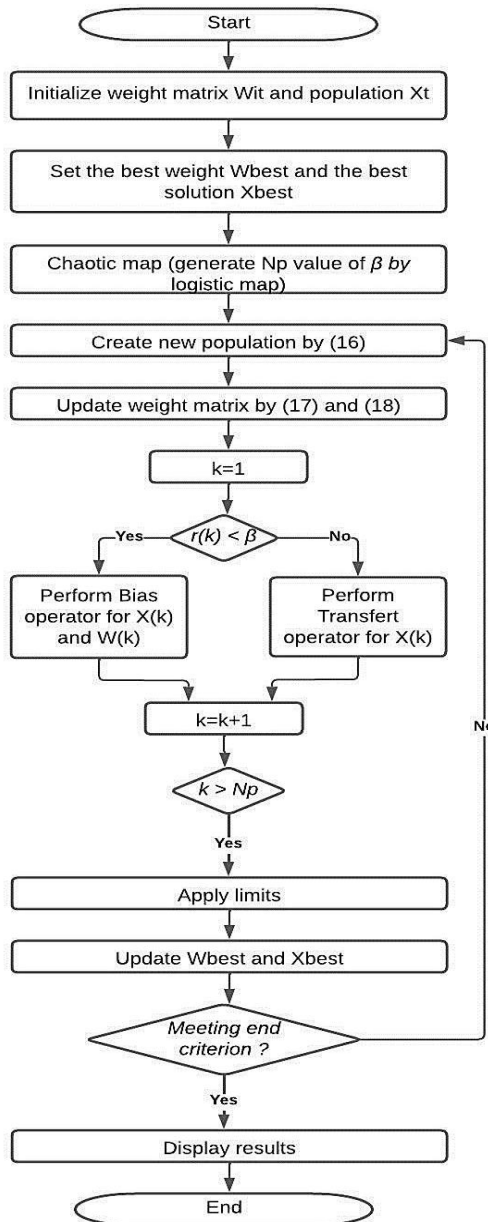
Figure 1. Flowchart of CNNA

4. SIMULATION RESULTS AND DISCUSSION

4.1. Assumptions

In this study, tests are performed for two cases:

a. #Case 1: Three DGs with unity PF (UPF-DG), in single-objective (minimization of ALI only), and in multi-objective (minimization of MOF).

b. #Case 2: Three DGs with optimal PF (OPF-DG), in single-objective (minimization of ALI only), and multi-objective (MOF minimization).

The main assumptions of this study are as: i) the load is considered constant and fixed at its nominal value; ii) the output power of the DGs is considered constant. The uncertainties related to solar irradiance or wind speed are not considered. Therefore, the characteristics of the DG system are not required in the main optimization program; iii) the insertion of DGs is considered without impact on the total harmonic distortion rate; iv) each node supports no more than one DG; and v) the inserted DGs are all equipped with an inverter, allowing them to operate in any PF. For simplicity, the present study considers only the case of DGs operating in type 1 or type 3.

The simulations in this study are conducted using MATLAB software version 2021a on a PC with an Intel(R) Core (TM) i5-3320M CPU running at 2.60 GHz and equipped with 4 CPUs, and 6GB RAM. The simulations are repeated 5 times with a population size of 40 and a maximum number of iterations set to 150. These settings are used consistently across all simulations to ensure accurate and reliable results. The load flow calculation program is based on the direct approach introduced by Teng [20].

4.2. IEEE 33-bus system

The IEEE 33-bus is a typical 32-branch RDS, introduced by Baran and Wu in [21]. The voltage at its reference node is equal to 12.66 kV with a base power of 100 MVA. The power rating of the total load is equal to 3,715 kW and 2,300 kVar. In the base case, this RDS has no devices. Herein, the load flow program estimates the active and reactive losses at 210.98 kW and 143 kVar.

4.2.1. Case 1

Table 1 summarizes all the results obtained for the 33-bus system in case 1. Herein, the total losses are reduced up to 65.5% in single-objective and 58.7% in multi-objective, which is respectively equivalent and superior to the results obtained by the recent hybrid algorithm SOS-NNA. In single-objective, the SOS-NNA proves a good local search capacity. Therefore, the results for the indices VD and VSI are slightly more refined compared to the CNNA. Besides, the choice of the weighting coefficients w_i in (9), can also increase the discrepancy between the obtained indices, but this always remains marginal. In addition, the minimum voltage of the network was increased from 0.9038 pu at bus 18 to 0.9809 pu at bus 25 in multi-objective optimization.

Table 1. Results for 33-bus system for three UPF-DGs in single-objective and in multi-objective (case 1)

Method	Locations	Sizes (kW)	Power loss (kW)/ Loss reduction (%)	VD	Minimum VSI	Minimum voltage (pu)/@ bus
			Single-objective			
Base case	-	-	210.98/0%	0.1337	0.6671	0.9038/18
Proposed	13	797.5	72.80/65.50%	0.0156	0.8782	0.9680/33
	30	1036.1				
	24	1089.7				
SCA [23]	13	827.3	72.83/65.48%	-	-	0.9680/33
	30	1082.15				
	24	1022.4				
NNA [15]	14	929.4	75.76/64.09%	0.01505	0.8804	-
	29	887.9				
	24	1009.2				
SOS-NNA [15]	13	801.8	72.78/65.50%	0.015113	0.88043	-
	30	1053.6				
	24	1091.3				
			Multi-objective			
Base case	-	-	210.98/0%	0.1337	0.6671	0.9038/18
Proposed	31	997.8	87.13/58.7%	0.00391	0.9258	0.9809/25
	14	937.2				
	6	1027.8				
SOS-NNA [15]	16	1123.4	95.79/54.6%	0.00339	0.9267	-
	24	1453.2				
	33	1138.6				

The results are also presented in Figure 2. The figure displays the convergence curves of both the single-objective and multi-objective scenarios, with the former displayed in Figure 2(a) and the latter depicted in Figure 2(b). The CNNA's ability to converge rapidly to a near-optimal solution is evident from the convergence curves, which highlights the algorithm's exploration capability.

In addition to the convergence curves, Figure 2 also displays the voltage profiles for both the single-objective and multi-objective scenarios. A comparison of Figures 2(a) and 2(b) shows a significant improvement in the voltage profile in the multi-objective case compared to the single-objective case. This is a further testament to the effectiveness of the CNNA in multi-objective integration of DGs into the RDS.

(a)   (b)
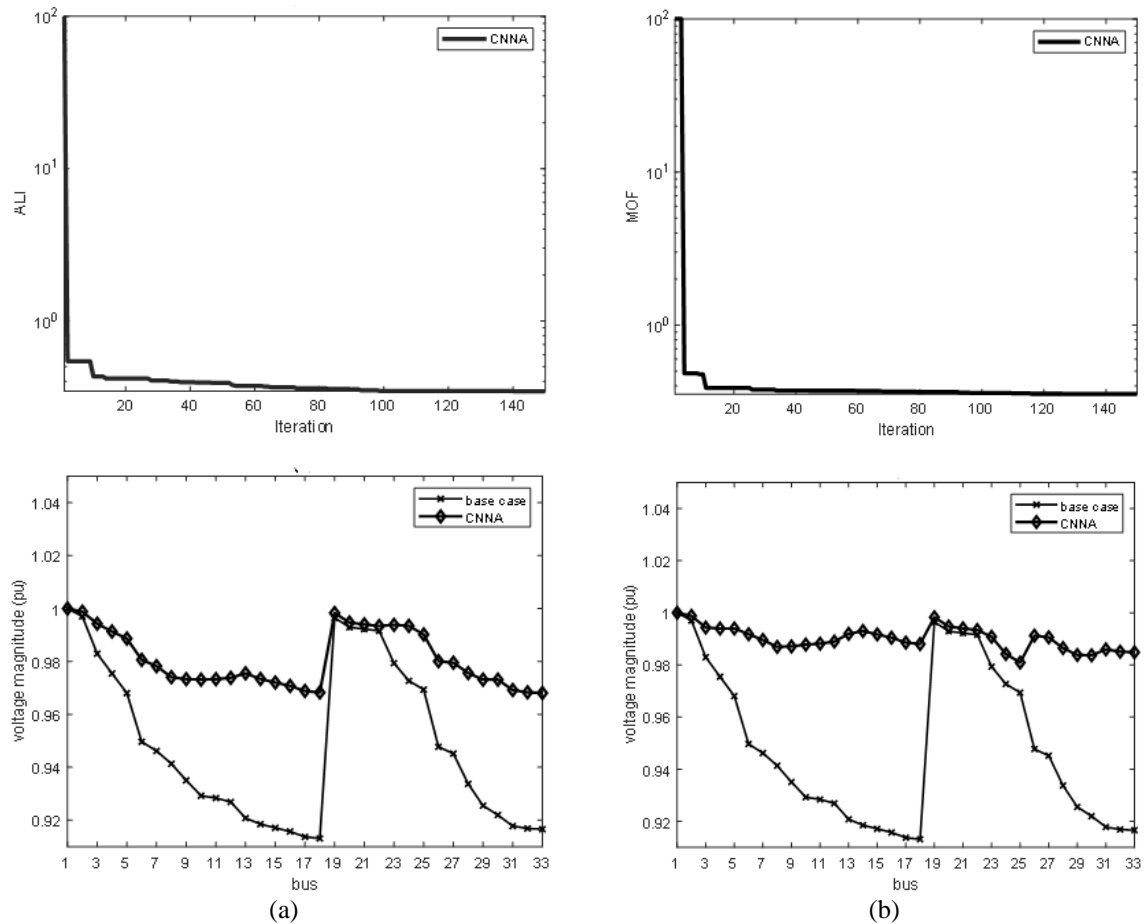
Figure 2. Convergence curve and voltage profile for 33-bus in case 1: three UPF-DGs (a) with single-objective and (b) with multi-objective

4.2.2. Case 2

Table 2 presents the outcomes acquired for case 2 of the 33-bus system. The results demonstrate a remarkable reduction in total losses, decreasing up to 93.66% in multi-objective optimization. Moreover, the VD is decreased to 0.000289 pu and the minimum voltage stability index (VSI) is enhanced to 0.9763 pu. These findings show that the proposed algorithm is highly effective in enhancing the problem dimension, particularly in multi-objective optimization. Notably, the results achieved through the proposed method exceed those attained by recent optimization methods, indicating the superior performance of the proposed algorithm.

The convergence curves in Figures 3(a) and 3(b) are used to assess the global search capability of the CNNA. These curves reveal that although the convergence rate is slow, the solutions generated by the algorithm are competitive with recent optimization methods. A comparison between the voltage profiles of the single-objective and multi-objective scenarios in Figures 3(a) and 3(b) indicates a slight improvement in the latter. Furthermore, the voltage profile in case 2 in Figure 3 exhibits a marked enhancement in comparison to case 1 in Figure 2, underscoring the significance of the DG's power factor variation in achieving satisfactory outcomes.

Table 2. Results for 33-bus system for three OPF-DGs in single-objective and
in multi-objective (case 2)

Method	Locations	Sizes (kW)	Power loss (kW)/ Loss reduction (%)	VD	Minimum VSI	Minimum voltage (pu)/@ bus
			Single-objective			
Base case	-	-	210.98/0%	0.1337	0.6671	0.9038/18
Proposed	30	1,167 (0.800)	13.15/93.7%	0.00076	0.9637	0.9908/8
	24	712.4 (0.873)				
	14	906.1 (0.814)				
NNA [15]	12	809.1 (0.824)	21.1/89.99%	0.00081	0.9532	-
	25	497.8 (0.536)				
	30	1,275.1 (0.873)				
SOS-NNA [15]	13	793.9 (0.904)	11.74/94.44%	0.00063	0.9688	-
	24	1,070 (0.900)				
	30	1,029.7 (0.713)				
			Multi-objective			
Base case	-	-	210.98/0%	0.1337	0.6671	0.9038/18
Proposed	13	807 (0.878)	13.37/93.66%	0.000289	0.9763	0.9940/22
	30	1,173.1 (0.800)				
	24	975 (0.805)				
NNA [15]	13	711.6 (0.884)	25.38/87.97%	0.001078	0.9763	-
	24	536 (0.532)				
	30	1,660 (0.867)				
SOS-NNA [15]	13	817 (0.888)	14.554/93.1%	0.000315	0.9775	-
	24	1,433.2 (0.905)				
	30	1,116.5 (0.725)				

Figure 3. Convergence curve and voltage profile for 33-bus in case 2: three OPF-DGs (a) with single-objective and (b) with multi-objective

4.3. IEEE 69-bus system

The typical IEEE 69-bus RDS is introduced by the same authors of the IEEE 33-bus [22]. It has 68 branches with base values equal to 12.66 kV and 100 MVA. The nominal power injected is equal to 3,800 kW and 2,690 kVar. In the base case, the active and reactive losses are estimated at 225 kW and 102.16 kVar.

4.3.1. Case 1

The effectiveness of the CNNA algorithm in the 69-bus system is demonstrated through Table 3, which reveals favorable outcomes. Specifically, in the single-objective optimization scenario, the active losses are lowered by 69.08%. In the multi-objective optimization case, the minimum VSI is increased to 0.9605 pu, and the active losses and VD are reduced to 67.28% and 0.00133 pu, respectively. These results are notably competitive and have not been achieved in existing literature, indicating the strength and efficacy of the CNNA algorithm, particularly as the RDS size is increased.

Table 3. Results for 69-bus system for three UPF-DGs in single-objective and in multi-objective (case 1)

Method	Locations	Sizes (kW)	Power loss (kW)/ Loss reduction (%)	VD	Minimum VSI	Minimum voltage (pu)/@ bus
			Single-objective			
Base case	-	-	225/0%	0.13370	0.6671	0.9091/65
Proposed	11	434	69.55/69.08%	0.00567	0.9171	0.9785/65
	61	1723.5 381.5				
	19					
SCA [23]	15	567.6 49.08	71.77/68.11%	-	-	0.9783/65
	27	1749.33				
	61					
MGSA [24]	15	562.65 1190.1	71.90/-	-	-	-
	61	523.3				
	63					
SOS-NNA [15]	11	526.8	69.43/69.14%	0.005201	0.9185	-
	18	380.3				
	61	1719				
			Multi-objective			
Base case	-	-	225/0%	0.13370	0.6671	0.9091/65
Proposed	61	2024.7 607.3	73.62/67.28%	0.00133	0.9605	0.9899/65
	66	397.5				
	21					
MOSCA [25]	10	1155.7 205.74	157.64/-	-	0.7764	0.9384/-
	61	1322.8				
	63					
SOS-NNA [15]	20	102.5 849.5	91.37/59.38%	0.00400	0.9430	-
	44	1813.1				
	63					

Figure 4 offers additional validation for the effectiveness of the multi-objective DG placement in the RDS. A comparison of the voltage profile between the single-objective scenario (presented in Figure 4(a)) and the multi-objective scenario (depicted in Figure 4(b)) reveals a significant improvement in the latter, further emphasizing the advantages of the multi-objective approach. Additionally, the convergence curves in both Figures 4(a) and 4(b) exhibit the strong exploration capability of the CNNA algorithm, demonstrating its ability to provide accurate and efficient results. These results provide persuasive evidence that the integration of DG with a multi-objective framework leads to optimal solutions for DG placement in the RDS.

4.3.2. Case 2

The convergence curves and voltage profiles obtained by of the CNNA algorithm in case 2 for the 69-bus system are presented in Figure 5. The curves provide insight into the exploration and convergence capabilities of the algorithm and its ability to generate high-quality solutions. Figures 5(a) and 5(b) demonstrate that CNNA displays a strong exploration capability, albeit at the cost of a slower convergence rate, as the chaotic strategy helps avoid premature convergence and enhances the quality of the obtained solutions. Notably, an improvement in voltage profile was observed (Figures 5(a) and 5(b)), with the best profiles generated in case 2, highlighting the suitability of the OPF-DG for compensating for instabilities and power losses. These results provide compelling evidence of the effectiveness of the proposed algorithm in tackling multi-objective optimization problems and dealing with problems of higher dimensionality.
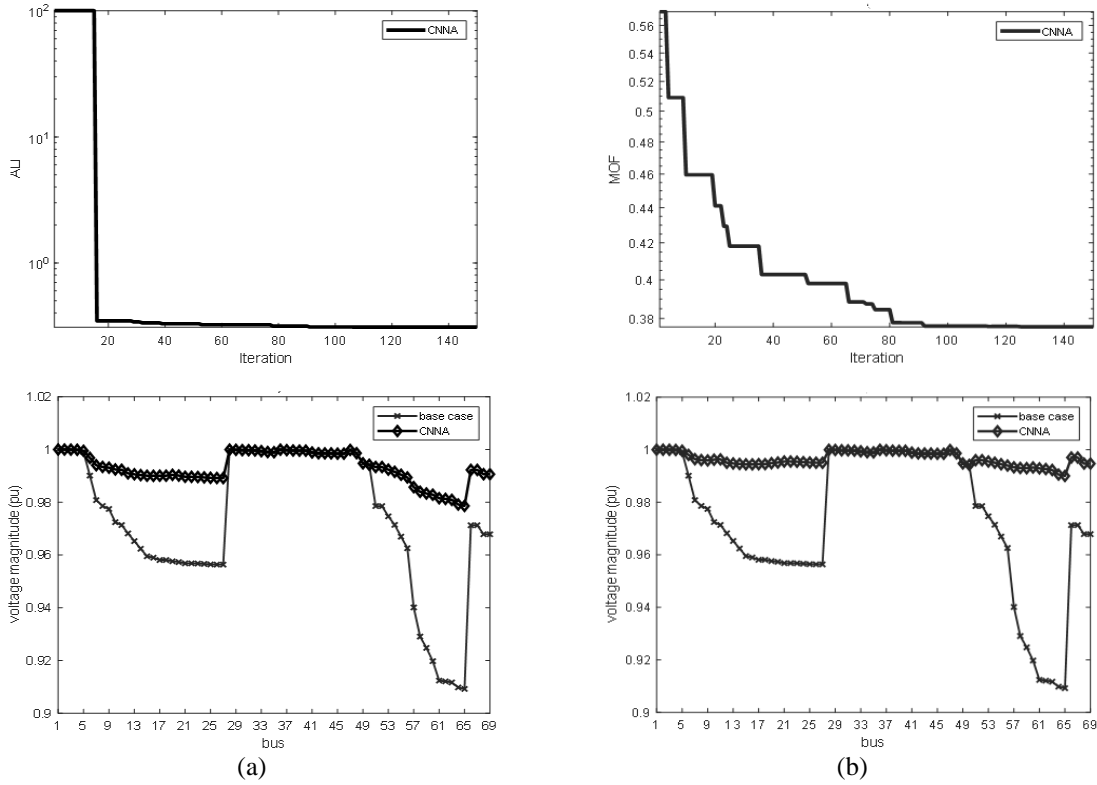
Figure 4. Convergence curve and voltage profile for 69-bus in case 1: three UPF-DGs (a) with single-objective and (b) with multi-objective
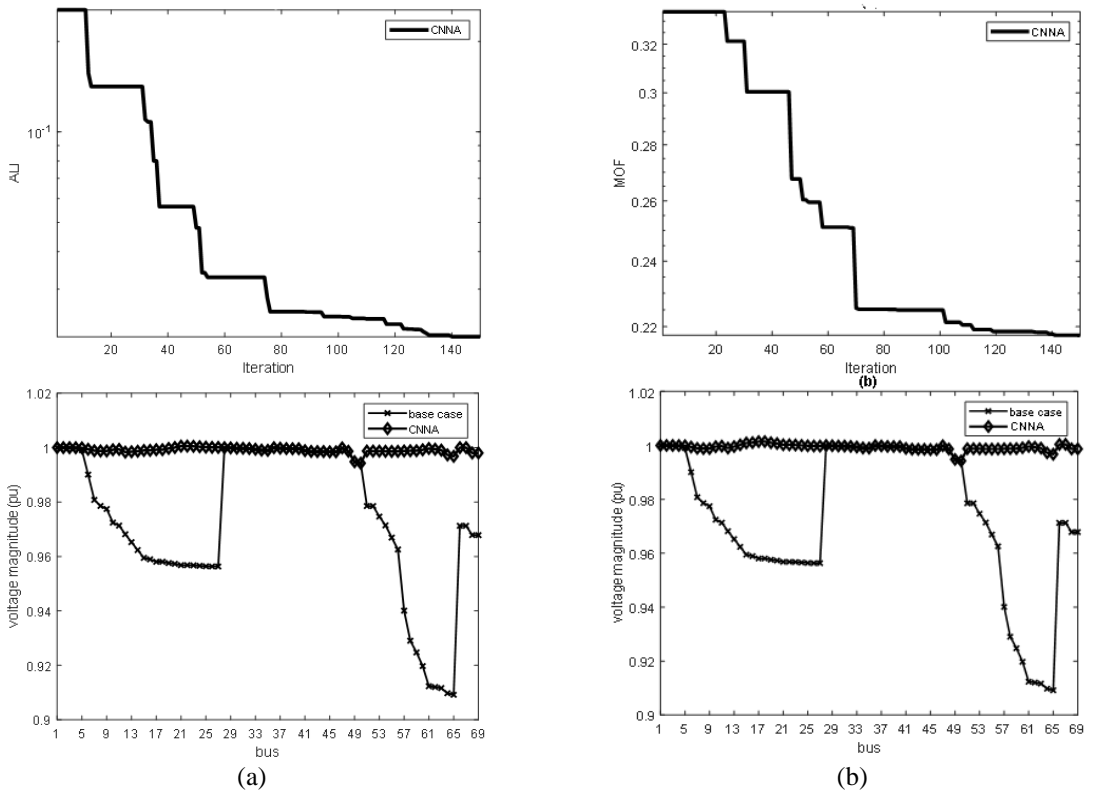

Figure 5. Convergence curve and voltage profile for 69-bus in case 2: three OPF-DGs (a) with single-objective and (b) with multi-objective

From Table 4, the results obtained by the CNNA are very impressive and show its robustness compared to other recent algorithms. The single-objective optimization showed a decrease in total losses to 98% while the multi-objective optimization showed a reduction in total losses to 97.5% and a decrease in voltage deviation to 0.000128 pu and an improvement in minimum VSI to 0.9772 pu. The results clearly demonstrate the superiority of the CNNA algorithm over SOS-NNA, especially with respect to the multi-objective resolution of the ODGA.

These results are a first in the literature and leave room for further improvements. The search space can be expanded by decreasing the severity of the constraints without compromising the safety and proper operation of the system. This can be tested taking into account load and generation uncertainties.

Table 4. Results for 69-bus system for three OPF-DGs in single-objective and in multi-objective (case 2)

Method	Locations	Sizes (kW) (PF)	Power loss (kW)/ Loss reduction (%)	VD	Minimum VSI	Minimum voltage (pu)/@ bus
			Single-objective			
Base case	-	-	225/0%	0.13370	0.6671	0.9091/65
Proposed	66	459.5 (0.800)	4.68/98%	0.000135	0.9772	0.9942/50
	61	1,672.3 (0.812)				
	21	380.2 (0.851)				
NNA [15]	9	1,092.1 (0.792)	17.63/92.2%	0.005974	0.9197	-
	37	582.3 (0.668)				
	62	1,592.1 (0.839)				
HHO [26]	17	270.8 (0.570)	6.58/97.1%	-	-	-
	61	1,541.4 (0.760)				
	66	696.8 (0.970)				
SOS-NNA [15]	11	493.5 (0.812)	4.27/98.1%	0.000127	0.9772	-
	18	380 (0.833)				
	61	1,674.3 (0.813)				
			Multi-objective			
Base case	-	-	225/0%	0.13370	0.6671	0.9091/65
Proposed	18	470.8 (0.947)	5.6/97.5%	0.000128	0.9772	0.9942/50
	67	480.6 (0.894)				
	61	1,664.2 (0.808)				
MOHHO [26]	15	332 (0.370)	21.8/90.3%	0.0008	0.980	-
	60	314 (0.35)				
	61	1,784 (0.980)				
MOIHHO [26]	13	1,064 (0.810)	13.9/93.83%	0.0005	0.9910	-
	49	1,235 (0.950)				
	62	1,610 (0.810)				
SOS-NNA [15]	16	608.3 (0.827)	6.59/97.06%	0.000297	0.9879	-
	49	1,192.8 (0.814)				
	61	1,835.9 (0.812)				

5. CONCLUSION

In this study, the solution to the ODGA problem is done through a chaotic neural networks algorithm CNNA. The efficiency of the CNNA is proved through its application on two typical systems, namely the IEEE 33-bus and the IEEE 69-bus. The simulations are done with three UPF-DGs for single and multi-objective optimization, as well as for three OPF-DGs. The results obtained show that the exploration capacity of the NNA has improved thanks to the Chao strategy. The results are quite competitive and superior to those obtained by existing methods in the literature, especially when the problem dimension is increased with a system having a large number of nodes such as the IEEE-69 bus. Hence, thanks to the CNNA a strong and optimal insertion of the DG can be ensured, without increasing the complexity of the optimization algorithm in space and time. Despite its remarkable performance, there are still areas for improvement. The CNNA shows a slight delay in convergence. Moreover, incorporating the generation and demand uncertainties, as well as expanding the system size, could lead to further optimization by the CNNA. Further research and improvement of the CNNA can enhance its capabilities and lead to solutions that are even more efficient.

REFERENCES

[1] M. Ruta, *The impact of the war in Ukraine on global trade and investment*. Washington: Open Knowledge, 2022.

[2] T. Haidi, B. Cheddadi, F. El Mariami, Z. El Idrissi, and A. Tarrak, "Wind energy development in Morocco: evolution and impacts," *International Journal of Electrical and Computer Engineering (IJECE)*, vol. 11, no. 4, pp. 2811–2819, Aug. 2021, doi: 10.11591/ijece.v11i4.pp2811-2819.

[3] C. Vezzoli *et al.*, *Designing sustainable energy for all*, 1st ed. Cham: Springer International Publishing, 2018.

[4] A. Tarraq, F. Elmariami, and T. Haidi, "Distributed renewable energy generation: a state-of-art of different planning methods,"

2019, doi: 10.13140/RG.2.2.12344.39686.

[5]   A. Rajendran and K. Narayanan, "Optimal installation of different DG types in radial distribution system considering load growth," *Electric Power Components and Systems*, vol. 45, no. 7, pp. 739–751, Apr. 2017, doi: 10.1080/15325008.2017.1309721.

[6]   A. S. Hassan, E. A. Othman, F. M. Bendary, and M. A. Ebrahim, "Optimal integration of distributed generation resources in active distribution networks for techno-economic benefits," *Energy Reports*, vol. 6, pp. 3462–3471, Nov. 2020, doi: 10.1016/j.egyr.2020.12.004.

[7]   S. Ganguly and D. Samajpati, "Distributed generation allocation with on-load tap changer on radial distribution networks using adaptive genetic algorithm," *Applied Soft Computing*, vol. 59, pp. 45–67, Oct. 2017, doi: 10.1016/j.asoc.2017.05.041.

[8]   A. Tarraq, F. Elmariami, A. Belfqih, and T. Haidi, "Meta-heuristic optimization methods applied to renewable distributed generation planning: a review," *E3S Web of Conferences*, vol. 234, Feb. 2021, doi: 10.1051/e3sconf/202123400086.

[9]   N. R. Bujal, M. Sulaiman, A. F. Abd Kadir, T. Khatib, and N. Eltawil, "A comparison between GSA and IGSA for optimal allocation and sizing of DG and impact to voltage stability margin in electrical distribution system," *Journal of Electrical Engineering and Technology*, vol. 16, no. 6, pp. 2949–2966, Nov. 2021, doi: 10.1007/s42835-021-00829-y.

[10]   K. Muthukumar and S. Jayalalitha, "Optimal placement and sizing of distributed generators and shunt capacitors for power loss minimization in radial distribution networks using hybrid heuristic search optimization technique," *International Journal of Electrical Power and Energy Systems*, vol. 78, pp. 299–319, Jun. 2016, doi: 10.1016/j.ijepes.2015.11.019.

[11]   E. S. Ali, S. M. Abd Elazim, and A. Y. Abdelaziz, "Ant lion optimization algorithm for optimal location and sizing of renewable distributed generations," *Renewable Energy*, vol. 101, pp. 1311–1324, Feb. 2017, doi: 10.1016/j.renene.2016.09.023.

[12]   I. A. Quadri, S. Bhowmick, and D. Joshi, "A comprehensive technique for optimal allocation of distributed energy resources in radial distribution systems," *Applied Energy*, vol. 211, pp. 1245–1260, Feb. 2018, doi: 10.1016/j.apenergy.2017.11.108.

[13]   L. Lopez, J. Doria-Garcia, C. Pimienta, and A. Arango-Manrique, "Distributed generation allocation and sizing: a comparison of metaheuristics techniques," in *2019 IEEE International Conference on Environment and Electrical Engineering and 2019 IEEE Industrial and Commercial Power Systems Europe*, Jun. 2019, pp. 1–6, doi: 10.1109/EEEIC.2019.8783934.

[14]   K. H. Truong, P. Nallagownden, I. Elamvazuthi, and D. N. Vo, "A Quasi-Oppositional-Chaotic symbiotic organisms search algorithm for optimal allocation of DG in radial distribution networks," *Applied Soft Computing*, vol. 88, Mar. 2020, doi: 10.1016/j.asoc.2020.106067.

[15]   T. P. Nguyen, T. A. Nguyen, T. V.-H. Phan, and D. N. Vo, "A comprehensive analysis for multi-objective distributed generations and capacitor banks placement in radial distribution networks using hybrid neural network algorithm," *Knowledge-Based Systems*, vol. 231, Nov. 2021, doi: 10.1016/j.knosys.2021.107387.

[16]   A. Selim, S. Kamel, and F. Jurado, "Voltage profile improvement in active distribution networks using hybrid WOA-SCA optimization algorithm," in *2018 Twentieth International Middle East Power Systems Conference (MEPCON)*, Dec. 2018, pp. 1064–1068, doi: 10.1109/MEPCON.2018.8635213.

[17]   S. Sannigrahi, S. Roy Ghatak, and P. Acharjee, "Multi-objective optimisation-based active distribution system planning with reconfiguration, intermittent RES, and DSTATCOM," *IET Renewable Power Generation*, vol. 13, no. 13, pp. 2418–2429, Oct. 2019, doi: 10.1049/iet-rpg.2018.6060.

[18]   T. Yuvaraj and K. Ravi, "Multi-objective simultaneous DG and DSTATCOM allocation in radial distribution networks using cuckoo searching algorithm," *Alexandria Engineering Journal*, vol. 57, no. 4, pp. 2729–2742, Dec. 2018, doi: 10.1016/j.aej.2018.01.001.

[19]   A. Sadollah, H. Sayyaadi, and A. Yadav, "A dynamic metaheuristic optimization model inspired by biological nervous systems: Neural network algorithm," *Applied Soft Computing*, vol. 71, pp. 747–782, Oct. 2018, doi: 10.1016/j.asoc.2018.07.039.

[20]   Jen-Hao Teng, "A direct approach for distribution system load flow solutions," *IEEE Transactions on Power Delivery*, vol. 18, no. 3, pp. 882–887, Jul. 2003, doi: 10.1109/TPWRD.2003.813818.

[21]   M. E. Baran and F. F. Wu, "Network reconfiguration in distribution systems for loss reduction and load balancing," *IEEE Transactions on Power Delivery*, vol. 4, no. 2, pp. 1401–1407, Apr. 1989, doi: 10.1109/61.25627.

[22]   M. E. Baran and F. F. Wu, "Optimal capacitor placement on radial distribution systems," *IEEE Transactions on Power Delivery*, vol. 4, no. 1, pp. 725–734, 1989, doi: 10.1109/61.19265.

[23]   A. Selim, S. Kamel, A. A. Mohamed, and E. E. Elattar, "Optimal allocation of multiple types of distributed generations in radial distribution systems using a hybrid technique," *Sustainability*, vol. 13, no. 12, Jun. 2021, doi: 10.3390/su13126644.

[24]   A. Eid, "Allocation of distributed generations in radial distribution systems using adaptive PSO and modified GSA multi-objective optimizations," *Alexandria Engineering Journal*, vol. 59, no. 6, pp. 4771–4786, Dec. 2020, doi: 10.1016/j.aej.2020.08.042.

[25]   A. Selim, S. Kamel, and F. Jurado, "Optimal allocation of distribution static compensators using a developed multi-objective sine cosine approach," *Computers and Electrical Engineering*, vol. 85, Jul. 2020, doi: 10.1016/j.compeleceng.2020.106671.

[26]   A. Selim, S. Kamel, A. S. Alghamdi, and F. Jurado, "Optimal placement of DGS in distribution system using an improved harris hawks optimizer based on single-and multi-objective approaches," *IEEE Access*, vol. 8, pp. 52815–52829, 2020, doi: 10.1109/ACCESS.2020.2980245.

BIOGRAPHIES OF AUTHORS

Ali Tarraq 🔟 📇 SC ⟳ was born in Safi, Morocco. He received the M. Eng. degree in industrial engineering from the University of Cadi Ayyad (UCA), National School of Applied Sciences, ENSA of Safi, Morocco, in 2010. Currently he is a Ph.D. student in electrical engineering at the National School of Electricity and Mechanics, ENSEM of Casablanca, Morocco. His current research interests include distributed generation based renewable energy, and smart grids applications. He can be contacted at email: ali.tarraq@gmail.com.

Faissal El Mariami ⬤ 🔳 SC ◓ is an engineer, Ph.D. and holder of university HDR accreditation. He is a professor qualified to direct research and member of the RECS research team at the National School of Electricity and Mechanics ENSEM (Hassan II University). Electrical networks stability and protection coordination are the center of his interest. He can be contacted at email: f_elmariami@yahoo.fr.

Abdelaziz Belfqih ⬤ 🔳 SC ◓ is an engineer, Ph.D. and holder of university HDR accreditation. He is a professor qualified to direct research and member of the RECS research team at the National School of Electricity and Mechanics ENSEM (Hassan II University). His research subjects focus on electrical networks and smart grids. He can be contacted at email: a-belfqih@hotmail.com.